nature immunology

BTLA is a lymphocyte inhibitory receptor with similarities to CTLA-4 and PD-1

Norihiko Watanabe[1,5], Maya Gavrieli[1], John R Sedy[1], Jianfei Yang[1,5], Francesca Fallarino[2], Susan K Loftin[1], Michelle A Hurchla[1], Natalie Zimmerman[3], Julia Sim[3], Xingxing Zang[4], Theresa L Murphy[1], John H Russell[3], James P Allison[4] & Kenneth M Murphy[1]

During activation, T cells express receptors for receiving positive and negative costimulatory signals. Here we identify the B and T lymphocyte attenuator (BTLA), an immunoglobulin domain–containing glycoprotein with two immunoreceptor tyrosine-based inhibitory motifs. BTLA is not expressed by naive T cells, but it is induced during activation and remains expressed on T helper type 1 (T_H1) but not T_H2 cells. Crosslinking BTLA with antigen receptors induces its tyrosine phosphorylation and association with the Src homology domain 2 (SH2)-containing protein tyrosine phosphatases SHP-1 and SHP-2, and attenuates production of interleukin 2 (IL-2). BTLA-deficient T cells show increased proliferation, and BTLA-deficient mice have increased specific antibody responses and enhanced sensitivity to experimental autoimmune encephalomyelitis. B7x, a peripheral homolog of B7, is a ligand of BTLA. Thus, BTLA is a third inhibitory receptor on T lymphocytes with similarities to cytotoxic T lymphocyte–associated antigen 4 (CTLA-4) and programmed death 1 (PD-1).

T cells receive costimulatory signals from antigen-presenting cells (APCs) that can be positive and negative. During the initiation of naive T cells, the primary positive costimulatory signal is mediated through the receptor CD28, whereas signaling through CTLA-4 has a negative effect on activation[1]. Both CD28 and CTLA-4 interact with the same set of ligands, B7-1 (also known as CD80) and B7-2 (CD86), expressed on APCs. Additional members of the CD28-B7 family have been identified. A second activating receptor on T cells is inducible costimulator (ICOS)[2], and its ligand B7h[3] (also known as B7RP-1 (ref. 4), GL50 (ref. 5), B7H2 (ref. 6) and LICOS[7]) is expressed on both lymphoid and nonlymphoid cells[8,9]. A second inhibitory receptor, PD-1 (refs. 10,11), binds to a pair of B7-related ligands PD-L1 (ref. 12), also known as B7-H1 (ref. 13), and PD-L2 (ref. 14), also known as B7-DC (ref. 15). B7-H3, another B7 homolog[16,17], binds an unidentified receptor on activated T cells.

Here we report the cloning and characterization of BTLA, an inhibitory receptor expressed by T lymphocytes. BTLA is induced on activation of naive T cells and is expressed by developing T_H1 and T_H2 cells. Expression of BTLA is subsequently lost on highly polarized T_H2 cells but remains on T_H1 cells. BTLA contains two cytoplasmic immunoreceptor tyrosine-based inhibitory motifs (ITIMs) and undergoes inducible tyrosine phosphorylation and association with SHP-1 and SHP-2. We show that coligation of BTLA partially inhibits CD3-induced secretion of IL-2 and that BTLA-deficient T cells have increased proliferation to antigen presented by dendritic cells (DCs), suggesting that BTLA exerts an inhibitory rather than activating influence on T cells. BTLA-deficient mice show a moderate increase in specific antibody response and an increased susceptibility to peptide antigen–induced experimental autoimmune encephalomyelitis (EAE), further suggesting an inhibitory role for BTLA. We also show that BTLA is recognized by an orphan B7 homolog, B7x. Thus, BTLA shares several structural and functional similarities with CTLA-4 and PD-1, the other two inhibitory receptors expressed on T lymphocytes.

RESULTS

Expression of BTLA mRNA

In a previous screen using Affymetrix arrays[18], we identified an anonymous T_H1-specific expressed sequence tag (EST). The full-length complementary DNA of this EST, cloned from a murine complementary DNA library (**Fig. 1** and **Supplementary Table 1** online), predicts a protein with a signal sequence, extracellular variable (V)-like immunoglobulin (Ig) domain, transmembrane region and intracellular domain of about 100 amino acids (**Fig. 1a**). By homology searching, we identified a single human gene homolog (**Fig. 1a,b**) with a similar domain structure. Notably, three tyrosine residues in the cytoplasmic domain are contained in sequence

[1]Department of Pathology & Immunology, Howard Hughes Medical Institute, Washington University School of Medicine, Box 8118, 660 South Euclid Avenue, St. Louis, Missouri 63110, USA. [2]Department of Experimental Medicine, University of Perugia, Via del Giochetto, 06122, Perugia, Italy. [3]Department of Molecular Biology & Pharmacology, Washington University School of Medicine, Box 8103, 660 South Euclid Avenue, St. Louis, Missouri, 63110, USA. [4]Howard Hughes Medical Institute, Department of Molecular and Cell Biology, Cancer Research Laboratory, University of California at Berkeley, Berkeley, California 94720, USA. [5]Present addresses: The Second Department of Internal Medicine, Chiba University School of Medicine, J1-8-1 Inohana, Chuo-ku, Chiba 260-8670, Japan (N.W.); Boehringer Ingelheim Pharmaceuticals, 900 Ridgebury Road, Ridgefield, Connecticut 06877, USA (J.Y.). Correspondence should be addressed to K.M.M. (murphy@immunology.wustl.edu).

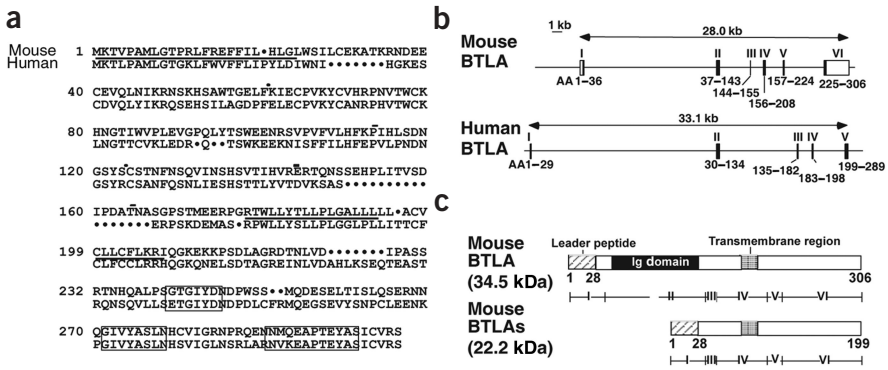

Figure 1 BTLA sequence and genomic structure. (**a**) Alignment of mouse and human BTLA. The signal peptide and the transmembrane region are underlined. Potential *N*-linked glycosylation sites (–) and cysteine residues (•) predicted to participate in disulfide bonds in the Ig domain are indicated. Spaces have been introduced for optimal comparison. Boxed sequences are tyrosine-based signaling motifs conserved between human and mouse BTLA, and are also conserved in the rat homolog (EST AI235902) expressed in normalized rat ovary. The mouse sequence is from the 129SvEv strain and the human sequence was cloned from the Ramos T cell line (Methods). (**b**) Exon and intron organization of mouse and human BTLA gene. Filled boxes indicate coding sequence in exons, and unfilled boxes indicate 3′ and 5′ untranslated regions. The amino acid number encoded by each exon is indicated below. (**c**) Predicted structural regions of mouse BTLA. Shown are full-length BTLA and a minor splice variant (BTLAs) that lacks exon 2 and thus the Ig domain. Roman numerals indicate the exon from which the predicted region is derived. The molecular weight of the predicted protein without posttranslational modifications is indicated in parentheses.

motifs that are conserved between mouse and human: the first is in a potential Grb2 interaction site[19] and the other two are in ITIM sequences[20]. In addition to BTLA, a minor alternatively spliced transcript, BTLAs, was detected by reverse transcription polymerase chain reaction (RT-PCR). BTLAs lacks exon 2 and thus the Ig domain (**Fig. 1c**).

BTLA mRNA is expressed strongly in spleen and lymph node tissues but very weakly or undetectably by several somatic tissues (**Fig. 2a**). It is expressed by both splenic B cell and T cells, with slightly higher levels in the former (**Fig. 2b**). By using an antigen-specific system to measure the expression of BTLA mRNA by northern analysis during T cell activation, we found low BTLA expression on day 2 after primary T cell activation, with no difference in expression between T_H1 and T_H2 conditions (**Fig. 2c**). On day 7 after primary T cell activation, expression of BTLA mRNA was increased, with slightly higher expression in T_H1 than in T_H2 cells (**Fig. 2c**). After a second week of *in vitro* culture under T_H1 or T_H2 polarization conditions, BTLA expression remained high in T_H1 cells, but by comparison was reduced in T_H2 cells (**Fig. 2d**).

Thus, expression of BTLA mRNA seems to be regulated during the activation and differentiation of T cells. BTLA expression is not strictly dependent on any single T_H1-inducing signal, because it remained expressed in T_H1 cells deficient for either signal transducer and activator of transcription 1 (STAT1) or STAT4. The A20 B cell line, but not macrophages or lymphokine activated killer (LAK) cells, also expressed BTLA mRNA (**Fig. 2b**).

BTLA surface expression and phosphorylation

To determine whether BTLA is a transmembrane protein, we expressed three forms of BTLA tagged with the Myc epitope in the Bjab cell line (**Fig. 3a**). Cell surface expression of wild-type BTLA was detected as predicted (**Fig. 3a**, top). Notably, deleting either the cytoplasmic or the Ig domain increased surface expression, suggesting that these domains have roles in controlling the amount of surface expression, similar to the regulation of surface CTLA-4 by its cytoplasmic domain[21,22].

Next, we confirmed that BTLA is a glycoprotein (**Fig. 3b**). Treatment with peptide *N*-glycosidase F (PNGase F) reduced the apparent molecular weight of both human and murine BTLA, consistent with the

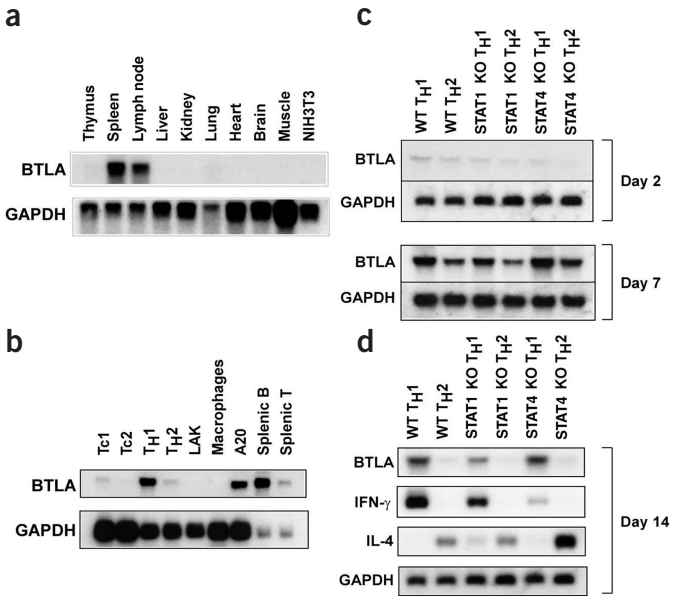

Figure 2 Expression of BTLA in lymphoid cells. (**a**) Tissue distribution of BTLA mRNA. Northern analysis of 10 μg of tissue or cellular RNA probed with full-length BTLA or GAPDH cDNA. (**b**) Northern analysis of total RNA from the indicated cells. Cytotoxic T cell type 1 (Tc1) and Tc2 cells were prepared from *in vitro*–polarized $2C^{51}$ TCR transgenic T cells, LAK cells were prepared by culturing C57BL/6 splenocytes with 1,000 U/ml of IL-2 for 9 d, and macrophages were from BALB/c bone marrow derived with L-cell conditioned media and confirmed as >95% Mac-1^+. Splenic B and T cells were purified to >98% by cell sorting. (**c**) Total RNA was isolated from T cells on days 2 and 7 after 3 h of incubation with PMA plus ionomycin, and northern blots were probed for BTLA and GAPDH mRNA. Data for days 2 and 7 are from blots that were hybridized and exposed together. (**d**) Expression of BTLA in polarized T_H1 and T_H2 cells on day 14. Wild-type, STAT1-deficient and STAT4-deficient DO11.10 transgenic T cells[18] (3×10^6 per ml) were activated by 0.3 μM OVA peptide in T_H1 or T_H2 conditions and again after 7 d in the same conditions. Cells were collected on day 14 and stimulated with PMA plus ionomycin for 3 h, and total RNA was analyzed for BTLA, IFN-γ, IL-4 and GAPDH mRNA as described[18].

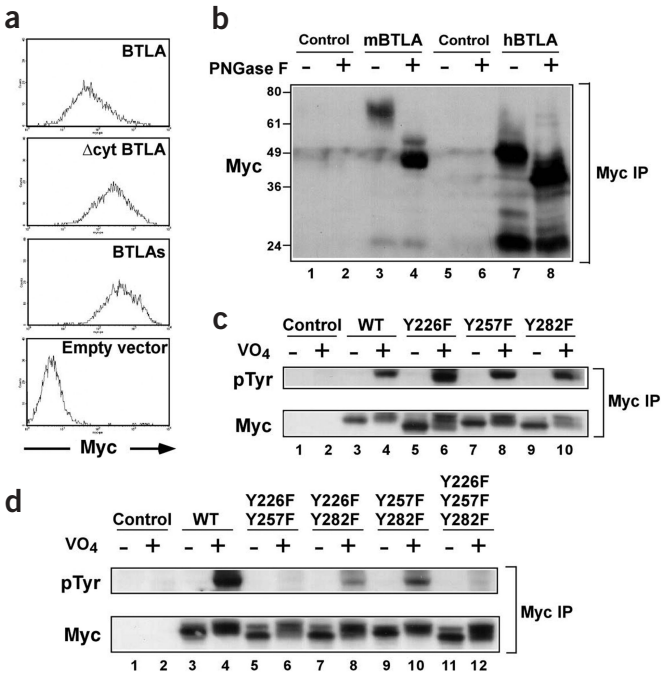

Figure 3 BTLA is transmembrane, glycoslyated, and tyrosine-phosphorylated on induction. (**a**) Transmembrane cell surface expression of BTLA. Bjab cells were infected with amphotrophic retrovirus containing empty vector, Myc_3-mBTLA-RV (BTLA), Δcyt-Myc_3-mBTLA-RV (Δcyt BTLA) and Myc_3-mBTLAs-RV (BTLAs). Expression of the Myc epitope was assayed on GFP-positive cells by FACS. (**b**) Murine and human BTLA contain *N*-linked oligosaccharides. A20 murine B lymphoma cells expressing control GFP-RV (lanes 1 and 2) or mBTLA-Myc_2-RV (lanes 3 and 4), and Bjab human B lymphoma cells expressing control GFP-RV (lanes 5 and 6) or hBTLA-Myc_3-RV (lanes 7 and 8) were prepared by infection with amphotrophic retrovirus, sorted for GFP expression and analyzed by immunoblotting (Methods). (**c**,**d**) Tyrosine phosphorylation of BTLA on stimulation with pervanadate. (**c**) Bjab cells infected with wild-type or single tyrosine mutants of hBTLA-Myc_3-RV were incubated in the absence (lanes 1, 3, 5, 7, 9) or presence (lanes 2, 4, 6, 8, 10) of pervanadate, and examined for tyrosine phosphorylation (Methods). (**d**) Bjab cells infected with double or triple tyrosine mutants of hBTLA-Myc_3-RV were analyzed for tyrosine phosphorylation (Methods).

N-linked glycosylation sites predicted in the extracellular region (**Fig. 1a**). The apparent molecular weight of human and murine BTLA treated with PNGase F was still higher than that predicted by its core amino acid sequence, suggesting that it has additional modifications such as *O*-linked glycosylation.

We also found that pervanadate treatment induced tyrosine phosphorylation of BTLA. Single mutation of tyrosines 226, 257 and 282 to phenylalanine had little effect on pervanadate-induced BTLA phosphorylation, but the triple tyrosine mutation blocked phosphorylation completely. The Y226F and Y257F double mutation severely reduced pervanadate-induced phosphorylation, suggesting that Y282 is either weakly phosphorylated or requires prior phosphorylation at Y226 or Y257 (**Fig. 3c**,**d**).

Thus, BTLA is an Ig domain-containing transmembrane glycoprotein that can be phosphorylated on tyrosines located in conserved cytoplasmic ITIM-like motifs.

Inducible SHP-1 and SHP-2 association

Sequences surrounding Y226 contain potential Grb2-binding motifs[23], Y257 seems to be an ITIM[20], and Y282 is similar to the immunoreceptor tyrosine-based switch motif (ITSM) in PD-1 (ref. 24) and SLAM (also called CD150 or IPO-3)[25]. To evaluate such potential interactions, we developed a system of inducible BTLA phosphorylation.

Extracellular Myc-tagged BTLAs was expressed stably in the DO11.10 hybridoma[26] (**Fig. 4a**). By a similar strategy to that used for crosslinking PD-1 with the B cell receptor complex[27], we crosslinked BTLA and the T cell antigen receptor (TCR) with antibodies to CD3 and the Myc epitope, and then carried out secondary crosslinking with goat anti–mouse IgG. Tyrosine phosphorylation of BTLA (**Fig. 4a**) was specific to BTLA-transduced cells, dependent on secondary crosslinking and not induced with anti-CD3 or anti-Myc alone (**Fig. 4a**,**b**). In addition, tyrosine phosphorylation of BTLA showed a time-dependent response: it appeared rapidly and peaked at 2–3 min, and was extinguished within 10 min of the secondary crosslinking (**Fig. 4a**).

We examined various signaling molecules for coimmunoprecipitation with Myc-BTLA. Notably, SHP-2 was strongly associated with BTLA. Association of SHP-2 correlated with phosphorylation of BTLA and was dependent on cocrosslinking (**Fig. 4a**, lanes 8–13). Pervanadate treatment also induced the association of SHP-2 with BTLA (**Fig. 4a**, lane 14), and this condition was used to examine further the association of BTLA with SHP-1 and SHP-2 (**Fig. 4c–e**). SHP-2 coprecipitated with pervanadate-treated BTLA (**Fig. 4c**,**d**, compare lanes 3 and 4). Coprecipitation of SHP-1 was also dependent on phosphorylation of BTLA (data not shown).

Inducible association of SHP-2 was also observed with human BTLA (**Fig. 4e**). Myc-tagged human BTLA was expressed in the human T cell line Jurkat. Myc-hBTLA coprecipitated with SHP-2 only in pervanadate-treated cells and was specific to expression of Myc-hBTLA (**Fig. 4e**). Likewise, only anti–SHP-2 immunoprecipitates from pervanadate-treated cells contained Myc-BTLA (**Fig. 4e**, lane 8). We also confirmed that SHP-1 associated with phosphorylated human BTLA (data not shown). The inducible association of BTLA with SHP-1 and SHP-2, a characteristic shared by CTLA-4 and PD-1, suggests that BTLA may have an inhibitory function in lymphocytes.

To explore the downstream effects of crosslinking BTLA with TCR, we examined the production of IL-2 in T cell hybridomas (**Fig. 4f**). Myc-tagged BTLA and BTLAs were stably expressed in DO11.10 hybridoma T cells[26]. Control DO11.10 hybridomas infected with the empty green fluorescent protein (GFP) retroviral vector, GFP-RV, showed anti-CD3–induced production of IL-2 that was unaffected by plate-bound anti-Myc (**Fig. 4f**). In contrast, production of IL-2 by DO11.10 cells expressing Myc-BTLA and Myc-BTLAs was dose-dependently inhibited by plate-bound anti-Myc (**Fig. 4f**). No differences in IL-2 production induced by phorbol 12-myristate 13-acetate (PMA) plus ionomycin were observed (**Fig. 4g**). Thus, it seems that BTLA can modestly inhibit antigen-induced, but not chemically induced, production of IL-2 by DO11.10 hybridoma cells.

Immune response in BTLA-deficient mice

To test whether BTLA has an inhibitory function *in vivo*, we targeted the *Btla* gene (**Fig. 5a**) to produce mice lacking BTLA (**Fig. 5b**). BTLA-deficient mice on a 129SvEv background lacked expression of BTLA

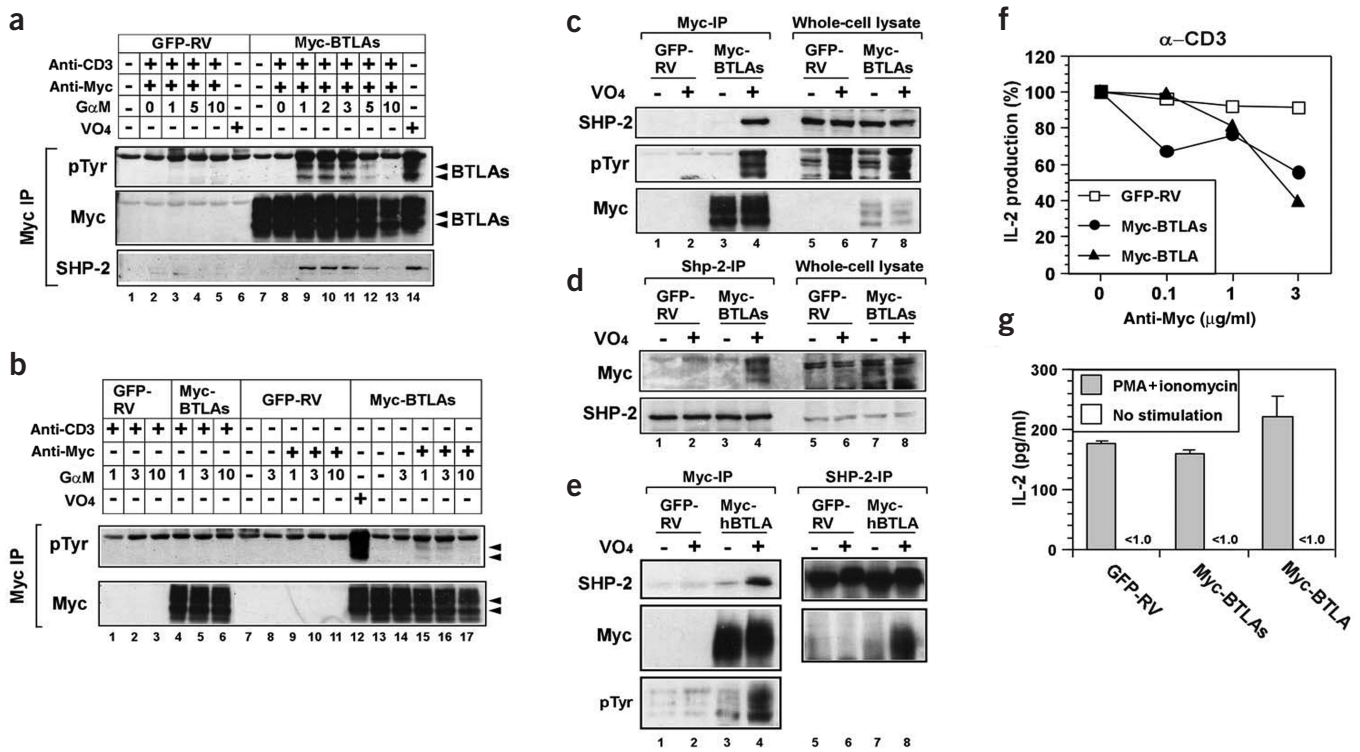

Figure 4 Inducible association of BTLA with SHP-2. (**a**) Tyrosine phosphorylation of BTLA on TCR crosslinking. DO11.10 hybridoma T cells were infected with empty vector (GFP-RV)[48] or Myc_3-mBTLAs-RV (Myc-BTLAs) and purified. After crosslinking (Methods), anti-Myc immunoprecipitates were analyzed with anti-pTyr (top), reprobed with polyclonal rabbit anti-Myc (middle), and then reprobed with rabbit anti–SHP-2 antibody (bottom). Arrowheads indicate the principal glycosylated forms of BTLAs. (**b**) BTLA tyrosine phosphorylation requires cocrosslinking. Cells in **a** were treated as indicated and analyzed for pTyr (top) or Myc (bottom). (**c**) Cells in **a** were incubated in the absence (–) or presence (+) of pervanadate for 2 min at 37 °C and lysed in 1% NP-40 lysis buffer. Anti-Myc immunoprecipitates and whole-cell lysates (25×10^6 cells) were analyzed sequentially for SHP-1 (data not shown), SHP-2, pTyr and Myc. (**d**) Cells were treated and lysed as in **c**. Anti–SHP-2 immunoprecipitates and whole-cell lysates were analyzed with anti-Myc (top), and reprobed with anti–SHP-2 (bottom). (**e**) Jurkat T cells were infected with GFP-RV or Myc_3-hBTLA-RV (hBTLA), sorted to >95% high surface expression of Myc-hBTLA, incubated in the absence (–) or presence (+) of pervanadate for 4 min at 37 °C, and lysed in 1% Triton X-100 lysis buffer. Anti-Myc (left) and anti–SHP-2 (right) immunoprecipitates were analyzed for Myc, SHP-2 and pTyr. (**f**,**g**) Crosslinking BTLA with TCR attenuates production of IL-2. DO11.10 cells expressing control vector (GFP-RV), Myc_3-mBTLAs-RV (Myc-BTLAs) or Myc_3-mBTLA-RV (Myc-BTLA) were stimulated with anti-CD3ε plus the indicated concentrations of anti-Myc (**f**) or with PMA plus ionomycin (**g**). The IL-2 concentration was determined by ELISA. In **f**, the IL-2 titer is normalized by the IL-2 concentration induced by stimulation with anti-CD3 alone.

mRNA in peripheral lymphocytes (**Fig. 5c**). No developmental defects in T or B cells in thymus or bone marrow were observed in these mice (**Supplementary Fig. 1** online). We produced BTLA-deficient DO11.10 TCR transgenic mice on a mixed 129SvEv and BALB/c background for the *in vitro* analysis of T cells (**Fig. 5d**). Fully polarized BTLA-deficient T_H1 cells showed a roughly twofold increase in proliferation in response to 0.3 μM OVA peptide presented by either $CD8^+$ or $CD8^-CD11c^+$ DCs (**Fig. 5d**).

We also examined T and B cells from wild-type and BTLA-deficient T cells for mitogen- and TCR-induced proliferation *in vitro* (**Fig. 6**). The proliferative response of wild-type and BTLA-deficient T cells to concanavalin A were comparable, but BTLA-deficient T cells showed a heightened response to stimulation with anti-CD3. Lipopolysaccharide (LPS)-induced proliferation was similar in wild-type and BTLA-deficient B cells, but BTLA-deficient B cells showed slightly greater responses to stimulation with anti-IgM. The increased *in vitro* responses, although not marked, were similar in magnitude to the increases in proliferation seen in PD-1-deficient T cells[11] and in CTLA-4-deficient $CD8^+$ T cells[28] *in vitro*. In fact, CTLA-4-deficient $CD4^+$ T cells show no enhancement of primary antigen-driven responses and only a twofold increase in secondary responses[29,30].

These results suggest that BTLA has an inhibitory, rather than activating, influence on T lymphocyte responses. Consistent with this, 4 weeks after immunization with nitrophenol-conjugated keyhole limpet hemocyanin (NP-KLH), BTLA-deficient mice showed a threefold increase in the amount of NP-KLH-specific IgG1, IgG2a and IgG2b isotypes as compared with control littermate 129/SvEv mice (**Table 1**).

EAE susceptibility in BTLA-deficient mice

As our data suggested that BTLA might be inhibitory, we used a model of EAE to detect potentially enhanced T cell responses in BTLA-deficient mice. Initially, we carried out an antigen dose titration of the myelin oligodendrocyte glycoprotein (MOG) peptide on the pure 129SvEv background to determine a dose that would generate a suboptimal disease capable of showing augmentation (**Fig. 7a**). We found that 10 μg and 50 μg of peptide induced severe disease in 129SvEv mice, whereas 2 μg induced milder disease with delayed onset (**Fig. 7a**). At this antigen dose, BTLA-deficient mice showed a higher incidence, increased clinical score, earlier onset and prolonged duration of disease as compared with wild-type littermate controls (**Fig. 7b**).

To ascertain any potential differences between the nature of MOG-induced EAE in BTLA-deficient mice and that in C57BL/6 control mice, we examined the lumbar spinal cords of affected mice (**Fig. 8**). There was an abundant cellular infiltrate in the lumbar spinal region of BTLA-deficient mice with a clinical score of 4, which was similar in severity to the infiltrate in C57BL/6 control mice induced with a high

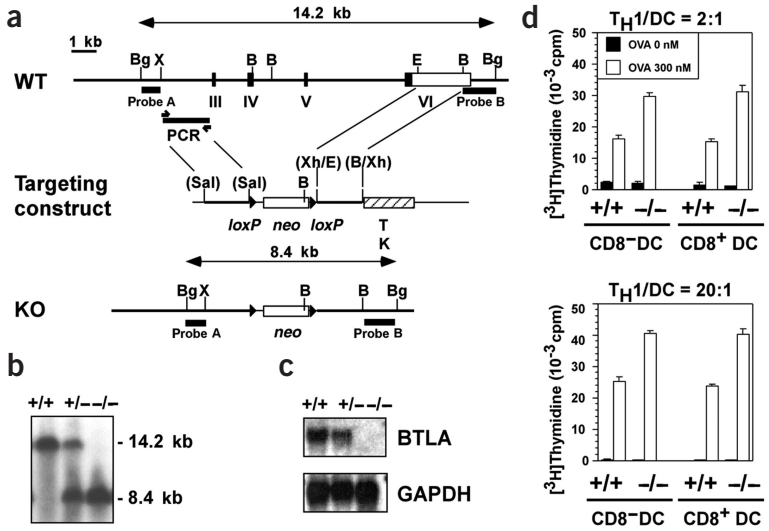

Figure 5 Generation and analysis of BTLA-deficient mice. (**a**) The *Btla* locus and targeting construct. Exons III–VI, encoding the extracellular, transmembrane and cytoplasmic regions, are indicated. *Bgl*II digestion of the germline locus generates a restriction fragment of 14.2 kb that hybridizes to probes A and B, and a fragment of 8.4 kb in correctly targeted clones. B, *Bam*HI; Bg, *Bgl*II; E, *Eco*RI; Sal, *Sal*I; X, *Xba*I; Xh, *Xho*I. TK, thymidine kinase gene; *neo*, neomycin resistance cassette. (**b**) Southern analysis. *Bgl*II-digested tail DNA hybridized with probe B. (**c**) Northern analysis. RNA was prepared directly from splenocytes of mice of the indicated genotype. Blots were hybridized to a full-length mouse BTLA cDNA probe, stripped and reprobed for GAPDH. (**d**) Proliferative responses of polarized T_H1 cells induced by incubation with antigen-pulsed DCs. Naive $CD4^+$ T cells from DO11.10 BTLA wild-type or BTLA-deficient mice were activated *in vitro* and passed biweekly in T_H1 conditions. Resting T_H1 cells (5×10^4) were incubated with BALB/c-derived $CD8^+$ or $CD8^-$ DCs (top, 2.5×10^4; bottom, 0.25×10^4), with or without 300 nM OVA peptide in a volume of 200 μl. Cell proliferation was measured by pulsing with [^{3}H]thymidine for 16 h.

dose of MOG peptide and also with a clinical score of 4 (compare **Fig. 8a** and **b**). Less abundant cellular infiltrates were observed in BTLA-deficient mice that were killed when the clinical score was 1.5 (**Fig. 8c**). Consistent with the MOG peptide–induced infiltrates observed in the C57BL/6 background[31], cellular infiltrates in BTLA-deficient mice consisted of both $CD4^+$ and $CD11b^+$ cells (**Fig. 8**), which were more frequent in mice with a clinical score of 4 than in those with a score of 1.5 (compare **Fig. 8f,g** and **d,e**).

Thus, loss of BTLA in 129SvEV mice increases the sensitivity to antigen-induced EAE, but the disease remains characterized by similar types of cellular infiltrate into the central nervous system (CNS).

BTLA interaction with a B7 homolog

The proposed similarity of BTLA to PD-1 and CTLA-4 is based primarily on the overall domain structure of the proteins, as each possesses a single extracellular Ig-like domain, a transmembrane region

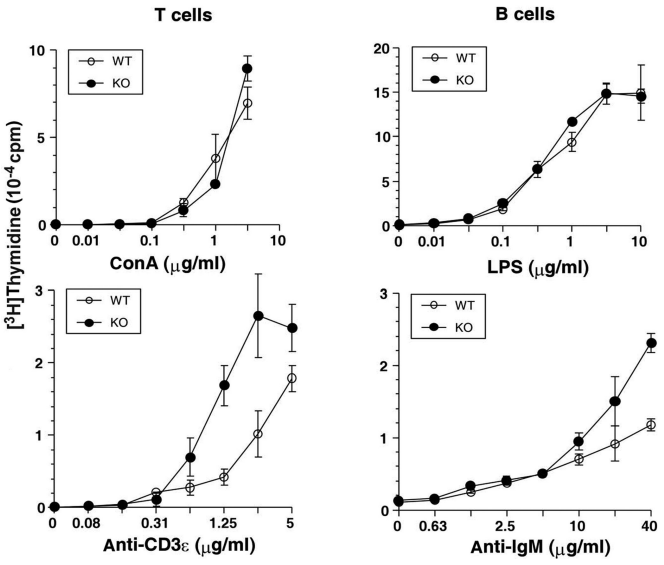

Figure 6 *In vitro* responses of BTLA-deficient lymphocytes. T and B cell from wild-type (WT) or BTLA-deficient (KO) mice were purified by cell sorting using anti-CD4–FITC, anti-CD8α–FITC or anti-B220–PE. Cells were stimulated with the indicated final concentrations of plate-bound anti-IgM, LPS, concanavalin A or plate-bound anti-CD3e. Cell proliferation was measured by pulsing with [^{3}H]thymidine for 16 h.

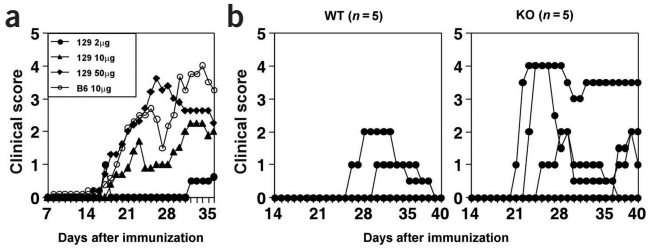

Figure 7 Increased EAE susceptibility in BTLA-deficient mice. (**a**) Titration of MOG peptide in 129SvEv mice. Mice were injected subcutaneously with MOG peptide at 2 μg, 10 μg and 50 μg ($n = 5$) in incomplete Freund's adjuvant and 500 μg of mycobacterium on day 0. Pertussis toxin (300 ng) of was injected intravenously on days 1 and 3. C57BL/6 (B6) mice injected with 10 μg of MOG were used as positive controls. Mice were monitored daily for symptoms. Clinical scores: 0, normal, no overt signs of disease; 1, limp tail or hindlimb weakness, but not both; 2, limp tail and hindlimb weakness; 3, partial hind limb paralysis; 4, complete hindlimb paralysis; 5, moribund state, death by EAE, killed for humane reasons. (**b**) Active induction of EAE by suboptimal dose of MOG peptide in BTLA-deficient mice. BTLA-deficient (KO) or wild-type (WT) littermate control 129SvEv mice aged 6–8 weeks ($n = 5$) were injected with 2 μg of MOG peptide as in **a**. Mean clinical scores: wild type, 0.6 ± 0.9; BTLA-deficient, 2.4 ± 1.7. Mean peak clinical score; wild type, 1.5 ± 0.7; BTLA-deficient 3.0 ± 1.2.

Table 1 Augmented IgG responses of BTLA-deficient mice to Td antigen

Anti-NP	*Btla*$^{+/+}$ (%)[a]	*Btla*$^{+/-}$ (%)	*Btla*$^{-/-}$ (%)
IgG1	157.9 ± 81.3	179.2 ± 160.6	272.1 ± 82.6[b]
IgG2a	110.0 ± 86.9	268.8 ± 203.9	306.7 ± 132.8[c]
IgG2b	92.51 ± 103.0	136.6 ± 38.8	249.8 ± 102.0[d]

[a]Data are presented as the percentage of mean isotype production as compared with wild-type BTLA serum, which was used as a uniform standard serum to determine relative titers of anti-NP. Data are the mean ± s.d. of measurements from five mice. [b]$P = 0.029$, [c]$P = 0.014$, [d]$P = 0.022$ versus wild-type BTLA.

and conserved intracellular ITIM motifs that interact with SHP-1 and SHP-2 phosphatases, and each has inhibitory rather than activating effects on lymphocytes. Both CTLA-4 and PD-1 interact with members of the B7 family[32], and we therefore tested whether BTLA also shares this feature. We identified a conserved B7 homolog, B7x, with high similarity between the mouse and human sequences. An alignment of human and murine B7x (**Supplementary Fig. 2** online) identified a predicted signal peptide and two Ig-like domains followed by a potential transmembrane region.

We generated a fusion protein of Ig and murine B7x and obtained additional Ig fusion proteins of B7h, PD-L1 and PD-L2. The B7h-Ig fusion protein showed no difference in binding between wild-type and BTLA-deficient T cells; this was expected, because B7h binds ICOS[3], which presumably should be expressed by both wild-type and BTLA-deficient T cells. In contrast, the B7x-Ig fusion protein bound to wild-type but not to BTLA-deficient T cells (**Fig. 9a**), suggesting that BTLA is responsible for most of the binding of B7x-Ig to T cells. PD-1 was expressed by both wild-type and BTLA-deficient T cells, but it was detected more strongly by anti–PD-1 than by the PD-L1 or PD-L2 Ig fusion proteins (**Fig. 9b,c**). In contrast, the B7-1 and B7-2 Ig fusion proteins generated stronger signals (**Fig. 9b**) on wild-type and BTLA-deficient T cells, consistent with the high affinity of CTLA-4 for B7-1 and B7-2.

Taken together, these results indirectly suggest that B7x is a ligand, although not necessarily the only ligand, for BTLA, thereby highlighting another similarity between BTLA and the other inhibitory receptors, CTLA-4 and PD-1, known to be expressed on T cells.

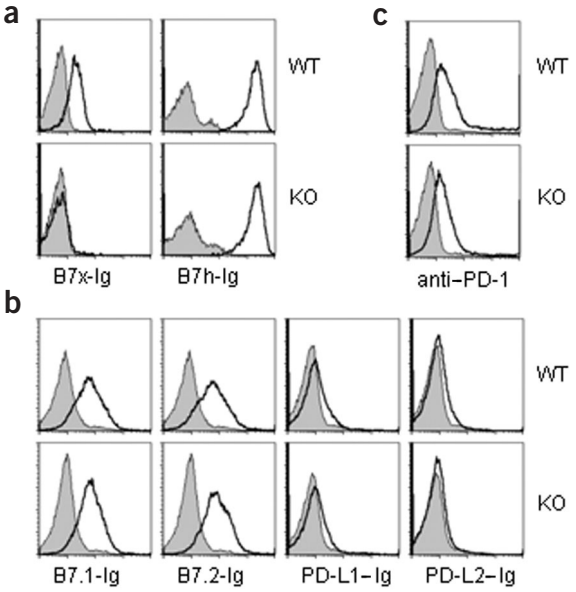

Figure 9 BTLA interacts with an orphan B7 B7x. (**a**) Spleen and lymph node cells from BTLA wild-type and BTLA-deficient DO11.10$^+$ TCR transgenic mice were collected and stimulated with 0.3 μM OVA peptide, 10 U/ml of IL-12 and neutralizing antibodies to IL-4, and assayed for Ig fusion binding after 4 d. Cells were stained with anti-CD4–FITC. Left, cells were stained with a human IgG1 antibody as a negative control (filled) or with a B7x-Ig fusion protein (open), followed by goat anti–human IgG–PE. Right, cells were unstained (filled) or stained with B7h-Ig (open), followed by biotinylated anti-Myc (murine IgG1 isotype) and streptavidin-PE. Anti-Myc was used as a negative control for the B7h-Ig fusion protein. (**b**,**c**) T_H1 cell lines derived from BTLA wild-type and BTLA-deficient DO11.10$^+$ mice were stimulated as above, collected on day 3, and assayed for binding to Ig fusion proteins. All cells were stained with anti-CD4–FITC. In **b**, Cells were stained with a human IgG1 antibody (filled) or with B7.1-Ig, B7.2-Ig, PD-L1–Ig and PD-L2–Ig fusion proteins (open), followed by goat anti–human Fcγ $F(ab')_2$–PE. In **c**, cells were stained with a hamster IgG2–PE as a negative control (filled) or with anti–PD-1–PE. Histograms are gated on CD4$^+$ cells.

DISCUSSION

BTLA seems to be a third inhibitory receptor expressed by T cells that, like PD-1, is induced on T cell activation but remains expressed more strongly on polarized T_H1 cells. Similar to PD-1 and CTLA-4 (ref. 27), BTLA can be induced to undergo phosphorylation and to associate with the SHP-1 and SHP-2 phosphatases by cocrosslinking with the TCR on T cells. The association with these phosphatases, the increased *in vivo* sensitivity to MOG peptide–induced EAE, and the increased rather than decreased *in vitro* proliferative responses suggest that

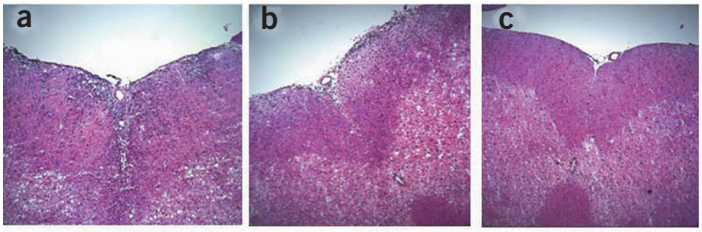

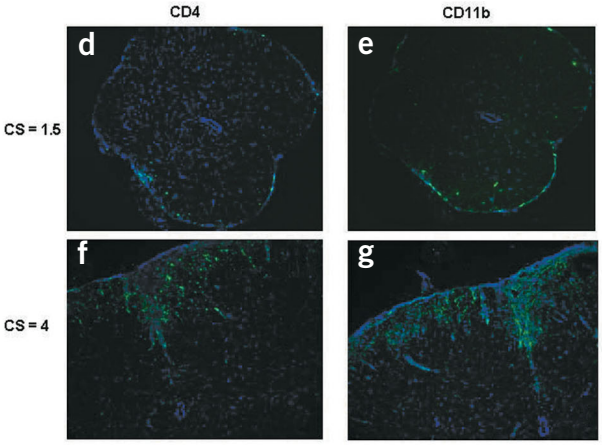

Figure 8 Infiltration of the CNS in MOG-induced EAE in BTLA-deficient mice. C57BL/6 control (**a**) or BTLA-deficient (**b**–**g**) mice immunized with MOG peptide were killed when showing the indicated clinical score (CS): (**a**) C57BL/6, CS 4; (**b**) BTLA-deficient, CS 4; (**c**-**e**) BTLA-deficient, CS 1.5; (**f**,**g**) BTLA-deficient, CS 4. Hematoxylin and eosin (**a**–**c**) or immunofluorescence staining for CD4 (left) and CD11b (right) (**d**–**g**) was done on frozen sections as described[31]. Immunofluorescent sections were counterstained with 4′,6-diamidino-2-phenylindole dihydrochloride (DAPI, blue).

BTLA may have an inhibitory function similar to that of PD-1 and CTLA-4, and may have a role in controlling late phases of immune responses and possibly autoimmunity.

The phenotypes generated by deficiencies in CTLA-4, PD-1 and BTLA suggest that PD-1 and BTLA may have partially redundant inhibitory signals. Of these three inhibitory receptors, deficiency in CTLA-4 produces by far the most marked *in vivo* phenotype[33]. In fact, the basis for spontaneous lymphoproliferative disease in CTLA-4-deficient mice is not fully understood, but it requires properties of the normal T cell repertoire *in vivo*, as it is abated or prevented when CTLA-4-deficient mice are crossed onto a TCR transgenic background[29] and delayed when crossed onto a FoxP3 transgenic background[34].

Antigen-specific proliferation or cytokine production in CTLA-4-deficient T cells is not enhanced during the primary response and shows modest, if any, increases during secondary responses[29,30]. This result indicates that the important inhibitory action of CTLA-4 is unlikely to be applied during the costimulation-dependent activation of T cells. Indeed, the greatest *in vitro* difference between wild-type and CTLA-4-deficient T cells occurs after the *in vivo* intravenous delivery of soluble antigen to induce anergy[30]. CTLA-4 may exert at least part of its regulatory activity by a non–cell-autonomous mechanism[35–37], contrary to the expected inhibitory action of SHP-1 or SHP-2 in cells expressing surface CTLA-4. A non–cell-autonomous inhibitory role for CTLA-4 might, for example, result from the engagement and crosslinking of B7 expressed by APCs[38], leading to an indirect regulatory action[39]. Thus, although CTLA-4 clearly has an important *in vivo* regulatory role, it is not yet totally clear how, when or where this action is exerted, or why no marked *in vitro* effect is seen.

In contrast to CTLA-4 deficiency, loss of PD-1 expression *in vivo* results in a phenotype that is variable and dependent on genetic background, being mild in 129SvEv mice[11] and more severe in BALB/c mice[40]. How the genetic background affects the requirement for PD-1 in regulating self-tolerance is not understood. *In vitro* analysis of PD-1-dependent T cell responses suggests that CD28-dependent, but not ICOS-dependent, costimulation overrides PD-1-dependent cellular inhibition[41]. In addition, inhibition by PD-1 of CD3-CD28–driven T cell activation is restricted to a very narrow range of activation; for example, it occurs at 1 μg/ml, but not at 2 μg/ml, of anti-CD3 *in vitro*[12] and is overcome by IL-2 (ref. 42). Thus, for both CTLA-4 and PD-1, the very modest effects seen in *in vitro* assays do not reflect the more marked and important actions of these inhibitory receptors observed *in vivo*.

In summary, whereas CTLA-4 deficiency produces a marked lymphoproliferative phenotype, PD-1 and BTLA deficiencies (on the 129SvEv background) individually produce a subtle phenotype characterized by enhanced propensity to autoimmunity. Although CTLA-4 can regulate both early events in T cell activation[43] and the later unfolding of autoimmunity[44,45], it seems that PD-1 and BTLA may function later in regulating effector responses, on the basis of their delayed expression in T cells. Conceivably, then, PD-1 and BTLA may have inhibitory actions that provide a redundant inhibitory system geared toward maintaining peripheral tolerance. An examination of mice deficient for both PD-1 and BTLA will be required to test this hypothesis.

CTLA-4 and PD-1 each interact with two known ligands, B7-1 and B7-2, and PD-L1 and PD-L2, respectively[32]. So far, we have identified only one candidate protein containing an Ig domain that may interact with BTLA. We may infer that an interaction occurs between BTLA and B7x from the loss of binding of the B7x-Ig fusion protein to BTLA-deficient T cells; however, it is conceivable that BTLA does not interact directly with the B7x-Ig fusion protein, but instead controls the expression of another, directly interacting, partner. On the basis of our interpretation that BTLA functions as an inhibitory receptor like PD-1 and CTLA-4, rather than as a regulator of protein transport, we favor the interpretation that there is a direct interaction between BTLA and B7x. Our analysis of potential BTLA-interacting candidates is in its early stages. So far, our search has been restricted to using Ig fusions of various B7 family members, which may limit the sensitivity of detecting interactions. For example, the limited sensitivity of Ig fusion proteins became evident in our control analysis of PD-1 expression. Anti–PD-1 detected a much higher signal that did the PD-L1 or PD-L2 Ig fusion proteins, probably a result of the lower affinities of the PD-L1 or PD-L2 Ig fusion proteins, as compared with the affinity of the PD-1 antibody, for PD-1. Thus, detecting additional BTLA-interacting proteins may require techniques with higher sensitivity.

The existence of a human homolog of BTLA that is very closely related to the mouse sequence, combined with the observation that murine and human BTLA cytoplasmic domains associate with the phosphatases SHP-1 and SHP-2, argue for a conserved inhibitory function. Polymorphisms in CTLA-4 may be linked to autoimmune disorders in humans[46,47]. Given the variable PD-1-deficient phenotype on different genetic backgrounds, and the quantitative nature of the BTLA-deficient phenotype, we propose that polymorphisms affecting the function of either of these inhibitory receptors could be a basis for variably penetrant susceptibility to autoimmunity in the human population. In this regard, we have noted variations among murine strains of the BTLA sequence (data not shown). Variations in receptor-ligand affinity, ligand expression or inherent receptor signaling could contribute to variable autoimmune susceptibility among individuals, particularly if these two inhibitory receptors provide a redundant shield for peripheral tolerance.

METHODS

Isolation of BTLA. We used an EST (aa839766) expressed by T_H1, but not T_H2, cells to screen a T_H1 cDNA phage library made in the Lambda ZAP vector (Stratagene) and isolated a partial clone, BTLAs, that lacked an Ig domain. Full-length BTLA cDNA, amplified from WEHI cell RNA by RT-PCR with primers J10-3K (5′-TTTGGCCTAAGATGCTGCTA-3′) and J10-7F (5′-CACA-GATTGGGTACGACATG-3′), was inserted into the GEM-T Easy Vector (Promega) to produce mJ11W1. We obtained additional full-length BTLA cDNA isolates by screening a second mouse splenocyte cDNA library (Stratagene) using the 5′ region of mj11W1 as a probe. Coding sequence and intron-exon boundaries were further determined by sequencing 129SvEv strain bacterial artificial chromosome clones containing the BTLA region (Genome Systems). Some Ig domain sequence polymorphisms occur among mouse strains. Human BTLA cDNA, amplified from Ramos B lymphoma RNA by RT-PCR with primers hJ10 (5′-TTTTCCATCACTGATATGTGCAGG-3′) and hJ10 AS (5′-GGTCCCTGTTGGAGTCAGAAAC-3′) based on the Celera human genome assembly, was inserted into the GEM-T Easy Vector to produce hJ11#14u.

Plasmid constructions. Myc-tagged BTLA constructs were prepared as follows. The open reading frame of mBTLAs was amplified from a colony obtained from screening a DO11.10 T_H1 cDNA library with primers J10-RV1-Bgl2 (5′-AGCTCTGAAGATCTCTAGGGAGGAAG-3′) and J10-Xho1 (5′-CATGCTC-GAGGAAGGTCCAGACAGAGGTATTG-3′). The product was digested with *Bgl*II and *Xho*I and cloned into the IRES-GFP-RV retrovirus[48] at the *Bgl*II and *Xho*I sites to produce mBTLAs-RV.

The N-terminal Myc-tagged version of mBTLAs (Myc_3-mBTLAs-RV) contains a triple Myc tag inserted downstream of the signal peptide. To produce this construct, a PCR product containing the mBTLA signal sequence and 3′ overhang homologous to the Myc tag was prepared with mBTLAs-RV as the template and primers J10-RV1-Bgl2 and J10-A2 (5′GTTCAGATCCAAGGAT-GCTCCAGAGGCCC-3′). This PCR product was annealed to a second PCR

product comprising three copies of the Myc epitope with 5′ and 3′ overhangs homologous to the N- and C-terminal portions of BTLA, respectively, which had been amplified from the triple Myc/Bluescript template with primers J10-A3 (5′-GAGCATCCTTGGATCTGAACAAAAGCTGATTA-3′) and J10-A4 (5′-CTTTCTCACAGAGCTCGTACAGGTCCTCT-3′). The triple Myc/Bluescript template contains 'anchor' sequences 5′ (GS) and 3′ (YEL) to the Myc_3 coding sequence, which are included in the final Myc-tagged mBTLA protein. We then amplified the two annealed pieces with primers J10-RV1-Bgl2 and J10-A4. This product was annealed to a third PCR product containing a 5′ Myc homologous tail and the C-terminal portion of BTLA amplified from the template mBTLAs-RV with primers J10-A5 (5′-GTACGAGCTCTGTGAGAAAGCTACTAA-GAGG-3′) and J10-Xho1, and the full-length chimeric cDNA was amplified with primers J10-RV1-Bgl2 and J10 Xho1. The resulting product was digested with *Bgl*II and *Xho*I and ligated into the *Bgl*II and *Xho*I sites of IRES-GFP-RV to yield Myc_3-mBTLAs-RV.

To produce the N-terminal Myc-tagged version of mBTLA (Myc_3-mBTLA-RV), primers J10-RV1-Bgl2 and J10-A4 were used to amplify the signal sequence linked to the triple Myc epitope from template Myc_3-mBTLAs-RV. A second PCR product was amplified with primers J10-A5 and J10 Xho1 and the template mJ11W1. The two PCR products were annealed and amplified with primers J10-RV1-Bgl2 and J10 Xho1, digested, and ligated into the retroviral vector to produce Myc_3-mBTLA-RV. A further modification was made by using the Quick Change mutagenesis kit (Stratagene) to convert a cysteine downstream of the Myc tag to alanine to mimic more accurately the predicted signal sequence processing in which this cysteine would be removed (SignalP V2.0).

Δcyt-Myc_3-mBTLA-RV was generated using Quick Change mutagenesis of Myc_3-mBTLA-RV with the primers mJ11 trunc top (5′-TGATATTCCATAAAC CTGCCACTGAGCCAG-3′) and mJ11 trunc bottom (5′-TGGCAGGTTTATG GAATATCAACCAGGTTAGTG-3′). mBTLA-Myc_2-RV, which expresses mBTLA with two C-terminal Myc epitopes, was generated by 'splicing by overlap extension' (SOEing) together two PCR products (generated from primers J10-RV1-Bgl2 and 3′ mj11 Myc tail (5′-GCTTTTGTTCACTTCTCACACAAATGGA TGC-3′) with template mJ11W1, and primers 5′ mjll Myc tail (5′-TGAGGAGTG AACAAAAGCTGATTAGCGAAG-3′) and new 3′ Xho Myc tail (5′-CCGCTCG AGCTCCTACAGGTCCTCTTC-3′) with template triple Myc/Bluescript) with primers J10-RV1-Bgl2 and new 3′ *Xho*I Myc tail and *Pfu* polymerase. After digestion with *Bgl*II and *Xho*I, the PCR product was ligated into the retroviral expression vector Tb-lym-GFP RV[49], which had been digested with *Bgl*II and *Xho*I, to generate mBTLA-Myc_2-RV.

The N-terminal Myc-tagged version of hBTLA containing a triple Myc tag inserted downstream of the signal peptide (Myc_3-hBTLA-RV) was prepared similarly. Three separate PCR products were generated using the following primers and templates: 5′ Bgl2 hj11 (5′-GAAGATCTGCAGGAAATGAAGACATTGCCT-3′) and 3′ Myc/hj11 bottom (5′-TCAGCTTTTGTTCCCCATGGATGTTCCA-GATGTCC-3′) with hj11#14u; 5′ hj11/Myc top (5′-CATCCATGGGGAACAAA AGCTGATTAGCGAAGAG-3′) and 3′ hj11/Myc bottom (5′-CACATGATTCTT TCAGGTCCTCTTCGCTAATCAGC-3′) with triple Myc/Bluescript; and 5′ Myc/hj11 top (5′-GAGGACCTGAAAGAATCATGTGATGTACAGCTTTA-3′) and 3′ Xho hj11 (5′-CCGCTCGAGTTGGAGTCAGAAACAGACTTAAC-3′) with hj11#14u. These PCR products were sequentially annealed and amplified, and cloned into tb-lym-GFP-RV, which had been digested with *Bgl*II and *Xho*I.

hBTLA containing three carboxy-terminal Myc epitopes (hBTLA-Myc_3-RV) was generated by SOEing together two PCR products (from primers 5′ Bgl2 hJ11 and 3′ hJ11 Myc tail (5′-TGAGGAGTGAACAAAAGCTGATTAGCGAAG-3′) with template hJ11#14u, and primers 5′ hj11 Myc tail (5′-TGAGGAGTGAA-CAAAAGCTGATTAGCGAAG-3′) and new 3′ Xho Myc tail with template triple Myc/Bluescript) with primers 5′ Bgl2 hJ11 and new 3′ Xho Myc tail and *Pfu* polymerase. After digestion with *Bgl*II and *Xho*I, the PCR product was ligated into retroviral expression vector Tb-lym-GFP-RV[49], which had been digested with *Bgl*II and *Xho*I, to generate hBTLA-Myc_3-RV. Embyronic stem cells (MC50) were a gift from R. Schreiber (Washington University School of Medicine, St. Louis, Missouri).

Tyrosine mutations. Single tyrosine-to-phenylalanine mutations of hBTLA-Myc_3-RV were produced using Quick Change mutagenesis and *Pfu* polymerase (Stratagene) with the following oligonucleotide pairs: Y226F top2 (5′-GA AACTGGAATTTATGATAATGACCCTGACCTTTG-3′) and Y226F bot (5′-GG GTCATTATCAAAAATTCCAGTTTCTGATAGCAG-3′); Y257F top2 (5′-ACCA GGCATTGTTTATGCTTCCCTGAACCATTCTG-3′) and Y257F bot (5′-AGG GAAGCAAAAACAATGCCTGGTTTGT-3′); Y282F top2 (5′-GCACCAACAG AATATGCATCCATATGTGTGAGG-3′) and Y282F bot (5′-ATATGGATGCAA ATTCTGTTGGTGCTTCTTTTA-3′).

We produced double and triple tyrosine-to-phenylalanine mutations of hBTLA-Myc_3-RV by using the oligonucleotide pair Y257F top2 and Y257F bot first with the Y226F-mutated hBTLA-Myc3-RV template to produce Y226F/Y257F and then with the Y282F-mutated template to produce Y257F/Y282F. The oligonucleotide pair Y282F top2 and Y282F bot was used with the Y226F-mutated template to produce Y226F/Y282F, and with the Y226F/Y257F-mutated template to produce Y226F/Y257F/Y282F.

Cell culture and expression analysis. Activation of DO11.10 TCR transgenic T cells[50] and retroviral infections, northern analysis and immunoblotting[49] were done as described. We prepared tissue and cellular RNA with the RNeasy Midi kit (Qiagen). A 20× stock of pervanadate was prepared 5 min before use by diluting 12.5 μl of 1 M $NaVO_4$ and 4 μl of 30% H_2O_2 to 600 μl in distilled water. The Opteia Mouse IL-2 set (PharMingen) was used to measure for IL-2 by enzyme-linked immunosorbent assay (ELISA).

Immunoblotting and analysis of *N*-linked glycosylation. To analyze the glycosylation status (**Fig. 3b**), cells (15×10^6 per ml) were lysed in Triton X-100 lysis buffer (25 mM HEPES (pH 7.5), 0.15 M NaCl, 1% Triton (v/v), 1 mM pervanadate, 1 μg/ml of leupeptin, 1 μg/ml of pepstatin, 1 μg/ml of aprotinin and 1 mM phenyl methylsulfonyl fluoride) for 30 min at 4 °C and centrifuged at 14,000*g* for 10 min. Extracts from 15×10^6 cells were immunoprecipitated with 1 μg of monoclonal antibodies to Myc (clone 9E10; Santa Cruz) and 20 μl of a 1:1 slurry of protein G–Sepharose (PGS) (Pharmacia). After being washed three times in Triton lysis buffer, the pellets were boiled for 10 min in 10 μl of PNGase denaturing buffer (NEB). After centrifugation to remove PGS, eluted proteins were transferred to PCR tubes containing 1 μl of 10% Nonidet P-40 (NP-40) and 1 μl of 10× G7 buffer (NEB), divided into two 6-μl aliquots, and treated without or with 1 μl of PNGase F (NEB) for 1 h at 37 °C. We boiled samples with 6 μl of 2× SDS-PAGE sample buffer and resolved them on 10% polyacrylamide gels. The proteins were transferred to nitrocellulose, blocked in 3% bovine serum albumin (BSA) in TBS-T buffer, blotted with rabbit anti-Myc (Santa Cruz) and horseradish peroxidase (HRP)-conjugated goat anti–rabbit IgG (Jackson), and analyzed by enhanced chemiluminescence (ECL).

To analyze the phosphorylation status (**Fig. 3c,d**), cells were treated with 1 mM pervanadate for 2 min at 37 °C, placed on ice for 1 min, lysed in an equal volume of 2× 1% Triton X-100 lysis buffer for 30 min and centrifuged for 10 min at 8,000*g*. Extracts from 15×10^6 cells were immunoprecipitated using 1 μg of anti-Myc (clone 9E10) and PGS. Blots were first analyzed for phosphotyrosine (pTyr) using HRP-conjugated (clone 4G10, Upstate Biotechnology), and then stripped and reanalyzed using rabbit anti-Myc and HRP-conjugated goat anti-rabbit IgG.

TCR crosslinking. To analyze the induction of tyrosine phosphorylation and association with SHP-1 and SHP-2 on TCR crosslinking, we infected DO11.10 hybridoma T cells with GFP-RV[48] or Myc_3-mBTLAs-RV and purified them by sorting. Cells were incubated with 4 μg/ml of hamster anti-CD3ε (clone 145-2C11, PharMingen) and 2 μg/ml of anti-Myc for 30 min at 4 °C, and crosslinked with 100 μg/ml of prewarmed goat anti–mouse IgG (GαM; Caltag) for various times, as indicated (**Fig. 4**). We used fluorescence-activated cell sorting (FACS) to confirm the cross-reactivity of goat anti–mouse IgG with hamster anti-CD3ε. As a positive control for phosphorylation, some cells were incubated with 1 mM pervanadate for 2 min at 37 °C. Cells were lysed in RIPA buffer, and 1 ml of lysates from 25×10^6 cells were immunoprecipitated with 2 μg of anti-Myc (9E10). We used the following antibodies to analyze the immunoprecipitates: anti-pTyr (RC20H, Transduction Laboratories), polyclonal rabbit anti-Myc (A-14, Santa Cruz), rabbit anti–SHP-2 (C-18, Santa Cruz), rabbit anti–SHP-1 antibody (C-19, Santa Cruz) and anti-Myc (9E10).

To measure the effect of crosslinking on IL-2 production, 3×10^4 DO11.10 cells expressing GFP-RV, Myc_3-mBTLAs-RV or Myc_3-mBTLA-RV were stimulated with 1 μg/ml of immobilized anti-CD3ε in combination with various concentrations of immobilized polyclonal rabbit anti-Myc or 50 ng/ml of PMA

plus 1 μM ionomycin. Culture supernatants of triplicate cultures were collected after 24 h, and the IL-2 concentration was determined by ELISA.

Antibody responses. Eight-week-old littermate wild-type, *Btla*$^{+/-}$ and *Btla*$^{-/-}$ mice on a pure 129SvEv background ($n = 5$) were injected intraperitoneally with 100 μg of NP^{17}-KLH (Biosearch Technologies) in alum (Pierce) on days 0 and 14. Sera was collected on day 28, and the titers of anti-NP were determined by ELISA using NP^{25}-BSA (Biosearch Technologies) for antibody capture and the SBA Clonotyping system/HRP kit for IgG subclass-specific ELISA (Southern Biotech).

***In vitro* responses of BTLA-deficient lymphocytes.** T and B cells from wild-type or BTLA-deficient mice were purified by cell sorting using fluorescein isothiocyanate (FITC)-conjugated anti-CD4 (Caltag), FITC-conjugated anti-CD8α (PharMingen) or phycoerythrin (PE)-conjugated anti-B220 (PharMingen). Cells (5×10^5 per ml) were stimulated with various concentrations of plate-bound anti-IgM (Affinipure F(ab′)$_2$ fragment goat anti–mouse IgM 115-006-075, Jackson ImmunoResearch), LPS (serotype 055:B5, Sigma), concanavalin A or plate-bound anti-CD3e (PharMingen, 145-2C11). Cell proliferation was measured after 48 h by pulsing with [^{3}H]thymidine for 16 h.

Production and interaction of B7x-Ig. In the public databases we identified a B7 homolog, B7x, that was conserved in mouse (accession code XP_143450.2 and AAH32925.1), rat (accession code XP_227553.1) and human (accession code NP_078902.1) and was highly conserved in sequence. B7x-Ig was prepared by fusing the coding region of the extracellular domain of B7x to the CH2-CH3 domain of mouse IgG1 and a Myc-His tag in pcDNA4 (a gift of W. Sha, Univ. California Berkeley, Berkeley, California, USA). The construct was linearized with *Bgl*II and transfected into 293T cells with FuGENE 6 (Roche). Stable transfectants were selected in 1 mg/ml of Zeocin (Invitrogen). To obtain fusion protein, we cultured stable transfectants in serum-free Dulbecco's modified Eagle's medium for 72 h, collected the supernatant and purified B7x-Ig by affinity column chromatography over His-Bind resin (Novagen). The purity of the fusion protein was confirmed by SDS-PAGE and by immunoblotting with antibodies against Myc and mouse IgG.

The following reagents were used to measure receptor and B7 ligand interactions (**Fig. 9**): anti-CD4–FITC (Caltag); human IgG1 antibody (Sigma); biotinylated anti-Myc (Santa Cruz); streptavidin-PE (PharMingen); B7.1-Ig, B7.2-Ig, PD-L1-Ig and PD-L2-Ig fusion proteins (Fc portion; human IgG1 isotype; R&D Systems); goat anti–human Fcγ F(ab′)$_2$–PE (Jackson ImmunoResearch); and anti–PD-1–PE (PharMingen).

FACS analysis. Human IgG1 and goat anti–human PE were gifts of M. Cella (Washington Univ., St. Louis, Missouri, USA). The construct for the B7h-Ig fusion protein[3], a gift of W. Sha (Univ. California Berkeley), and the cDNA encoding the fusion protein were inserted into the GFP-RV retroviral vector[48], and the retrovirus was used to infect J558 cells. We purified fusion protein from infected J558 supernatant with His-Bind resin (Novagen). B7.1-Ig, B7.2-Ig, PD-L1-Ig and PD-L2-Ig fusion proteins (Fc portion; human IgG1 isotype) were obtained from R&D Systems. All analyses were done on a FACSCalibur.

To measure the surface expression of BTLA, Bjab cells were infected with amphotrophic retrovirus prepared in Phoenix A packaging cells to express empty vector, Myc$_3$-mBTLA-RV, Δcyt-Myc$_3$-mBTLA-RV and Myc$_3$-mBTLAs-RV. Expression of the Myc epitope on GFP-positive cells was assayed on a FACScalibur with rabbit anti-Myc polyclonal serum (Santa Cruz) and PE-conjugated goat F(ab′)$_2$ anti–rabbit IgG (Jackson Research Laboratories).

Histological analysis. CNS tissues were removed from mice and frozen and 10-μm sections were prepared. Sections shown are from lumbar spinal cord. We prepared sections stained with hematoxylin and eosin, and measured the expression of CD4 and CD11b by immunofluorescence microscopy as described[31].

Accession codes. Murine BTLA, AY293285; human BTLA, AY293286; murine B7x, XP_14350.2 and AAH32925.1; rat B7x, XP_227553.1; human B7x, NP_078902.1 (http://www.ncbi.nlm.nih.gov/entrez/query.fcgi?db=protein). From the NCBI Protein database.

Note: Supplementary information is available on the Nature Immunology website.

ACKNOWLEDGMENTS
We thank B. Sleckman for help with gene targeting; M. White for generating chimeric mice; M. Gimenez for help with immunohistochemistry; and W. Sha for discussions. This work was supported in part by grants from the National Institutes of Health. J.P.A. and K.M.M. are Investigators of the Howard Hughes Medical Institute.

COMPETING INTERESTS STATEMENT
The authors declare that they have no competing financial interests.

Received 13 January; accepted 13 May 2003
Published online 8 June 2003; doi:10.1038/ni944

1. Coyle, A.J. & Gutierrez-Ramos, J.C. The expanding B7 superfamily: increasing complexity in costimulatory signals regulating T cell function. *Nat. Immunol.* **2**, 203–209 (2001).
2. Hutloff, A. *et al.* ICOS is an inducible T-cell co-stimulator structurally and functionally related to CD28. *Nature* **397**, 263–266 (1999).
3. Swallow, M.M., Wallin, J.J. & Sha, W.C. B7h, a novel costimulatory homolog of B7.1 and B7.2, is induced by TNFα. *Immunity* **11**, 423–432 (1999).
4. Yoshinaga, S.K. *et al.* T-cell co-stimulation through B7RP-1 and ICOS. *Nature* **402**, 827–832 (1999).
5. Ling, V. *et al.* Cutting edge: identification of GL50, a novel B7-like protein that functionally binds to ICOS receptor. *J. Immunol.* **164**, 1653–1657 (2000).
6. Wang, S. *et al.* Costimulation of T cells by B7-H2, a B7-like molecule that binds ICOS. *Blood* **96**, 2808–2813 (2000).
7. Brodie, D. *et al.* LICOS, a primordial costimulatory ligand? *Curr. Biol.* **10**, 333–336 (2000).
8. Liang, L. & Sha, W.C. The right place at the right time: novel B7 family members regulate effector T cell responses. *Curr. Opin. Immunol.* **14**, 384–390 (2002).
9. Liang, L., Porter, E.M. & Sha, W.C. Constitutive expression of the B7h ligand for inducible costimulator on naive B cells is extinguished after activation by distinct B cell receptor and interleukin 4 receptor–mediated pathways and can be rescued by CD40 signaling. *J. Exp. Med.* **196**, 97–108 (2002).
10. Ishida, Y. *et al.* Induced expression of PD-1, a novel member of the immunoglobulin gene superfamily, upon programmed cell death. *EMBO J.* **11**, 3887–3895 (1992).
11. Nishimura, H. *et al.* Immunological studies on PD-1 deficient mice: implication of PD-1 as a negative regulator for B cell responses. *Int. Immunol.* **10**, 1563–1572 (1998).
12. Freeman, G.J. *et al.* Engagement of the PD-1 immunoinhibitory receptor by a novel B7 family member leads to negative regulation of lymphocyte activation. *J. Exp. Med.* **192**, 1027–1034 (2000).
13. Dong, H. *et al.* B7-H1, a third member of the B7 family, co-stimulates T-cell proliferation and interleukin-10 secretion. *Nat. Med.* **5**, 1365–1369 (1999).
14. Latchman, Y. *et al.* PD-L2 is a second ligand for PD-l and inhibits T cell activation. *Nat. Immunol.* **2**, 261–268 (2001).
15. Tseng, S.Y. *et al.* B7-DC, a new dendritic cell molecule with potent costimulatory properties for T cells. *J. Exp. Med.* **193**, 839–846 (2001).
16. Chapoval, A.I. *et al.* B7-H3: a costimulatory molecule for T cell activation and IFN-γ production. *Nat. Immunol.* **2**, 269–274 (2001).
17. Sun, M. *et al.* Characterization of mouse and human B7-H3 genes. *J. Immunol.* **168**, 6294–6297 (2002).
18. Yang, J. *et al.* IL-18-stimulated GADD45β required in cytokine-induced, but not TCR-induced, IFN-γ production. *Nat. Immunol.* **2**, 157–164 (2001).
19. Tomasello, E. *et al.* Signaling pathways engaged by NK cell receptors: double concerto for activating receptors, inhibitory receptors and NK cells. *Semin. Immunol.* **12**, 139–147 (2000).
20. Bolland, S. & Ravetch, J.V. Inhibitory pathways triggered by ITIM-containing receptors. *Adv. Immunol.* **72**, 149–177 (1999).
21. Shiratori, T. *et al.* Tyrosine phosphorylation controls internalization of CTLA-4 by regulating its interaction with clathrin-associated adaptor complex AP-2. *Immunity* **6**, 583–589 (1997).
22. Zhang, Y. & Allison, J.P. Interaction of CTLA-4 with AP50, a clathrin-coated pit adaptor protein. *Proc. Natl. Acad. Sci. USA* **94**, 9273–9278 (1997).
23. Songyang, Z. *et al.* Specific motifs recognized by the SH2 domains of Csk, 3BP2, fps/fes, GRB-2, HCP, SHC, Syk, and Vav. *Mol. Cell. Biol.* **14**, 2777–2785 (1994).
24. Nishimura, H. *et al.* Development of lupus-like autoimmune diseases by disruption of the PD-1 gene encoding an ITIM motif-carrying immunoreceptor. *Immunity* **11**, 141–151 (1999).
25. Shlapatska, L.M. *et al.* CD150 association with either the SH2-containing inositol phosphatase or the SH2-containing protein tyrosine phosphatase is regulated by the adaptor protein SH2D1A. *J. Immunol.* **166**, 5480–5487 (2001).
26. Haskins, K. *et al.* The major histocompatibility complex–restricted antigen receptor on T cells. I. Isolation with a monoclonal antibody. *J. Exp. Med.* **157**, 1149–1169 (1983).
27. Okazaki, T. *et al.* PD-1 immunoreceptor inhibits B cell receptor–mediated signaling by recruiting Src homology 2-domain-containing tyrosine phosphatase 2 to phosphotyrosine. *Proc. Natl. Acad. Sci. USA* **98**, 13866–13871 (2001).
28. Chambers, C.A. *et al.* Secondary but not primary T cell responses are enhanced in CTLA-4-deficient CD8$^+$ T cells. *Eur. J. Immunol.* **28**, 3137–3143 (1998).

29. Oosterwegel, M.A. *et al.* The role of CTLA-4 in regulating Th2 differentiation. *J. Immunol.* **163**, 2634–2639 (1999).
30. Greenwald, R.J. *et al.* CTLA-4 regulates induction of anergy *in vivo*. *Immunity* **14**, 145–155 (2001).
31. Sabelko-Downes, K.A., Cross, A.H. & Russell, J.H. Dual role for Fas ligand in the initiation of and recovery from experimental allergic encephalomyelitis. *J. Exp. Med.* **189**, 1195–1205 (1999).
32. Sharpe, A.H. & Freeman, G.J. The B7-CD28 superfamily. *Nat. Rev. Immunol.* **2**, 116–126 (2002).
33. Tivol, E.A. *et al.* Loss of CTLA-4 leads to massive lymphoproliferation and fatal multiorgan tissue destruction, revealing a critical negative regulatory role of CTLA-4. *Immunity.* **3**, 541–547 (1995).
34. Khattri, R. *et al.* An essential role for Scurfin in CD4+CD25+ T regulatory cells. *Nat. Immunl.* **4**, 337–342 (2003).
35. Bachmann, M.F. *et al.* Cutting edge: lymphoproliferative disease in the absence of CTLA-4 is not T cell autonomous. *J. Immunol.* **163**, 1128–1131 (1999).
36. Bachmann, M.F. *et al.* Normal pathogen-specific immune responses mounted by CTLA-4-deficient T cells: a paradigm reconsidered. *Eur. J. Immunol.* **31**, 450–458 (2001).
37. Tivol, E.A. & Gorski, J. Re-establishing peripheral tolerance in the absence of CTLA-4: complementation by wild-type T cells points to an indirect role for CTLA-4. *J. Immunol.* **169**, 1852–1858 (2002).
38. Grohmann, U. *et al.* CTLA-4-Ig regulates tryptophan catabolism *in vivo*. *Nat. Immunol.* **3**, 1097–1101 (2002).
39. Finger, E.B. & Bluestone, J.A. When ligand becomes receptor—tolerance via B7 signaling on DCs. *Nat. Immunol.* **3**, 1056–1057 (2002).
40. Nishimura, H. *et al.* Autoimmune dilated cardiomyopathy in PD-1 receptor–deficient mice. *Science* **291**, 319–322 (2001).
41. Bennett, F. *et al.* Program death-1 engagement upon TCR activation has distinct effects on costimulation and cytokine-driven proliferation: attenuation of ICOS, IL-4, and IL-21, but not CD28, IL-7, and IL-15 responses. *J. Immunol.* **170**, 711–718 (2003).
42. Carter, L. *et al.* PD-1:PD-L inhibitory pathway affects both CD4+ and CD8+ T cells and is overcome by IL-2. *Eur. J. Immunol.* **32**, 634–643 (2002).
43. Brunner, M.C. *et al.* CTLA-4-mediated inhibition of early events of T cell proliferation. *J. Immunol.* **162**, 5813–5820 (1999).
44. Luhder, F. *et al.* Cytotoxic T lymphocyte-associated antigen 4 (CTLA-4) regulates the unfolding of autoimmune diabetes. *J. Exp. Med.* **187**, 427–432 (1998).
45. Luhder, F. *et al.* Pinpointing when T cell costimulatory receptor CTLA-4 must be engaged to dampen diabetogenic T cells. *Proc. Natl. Acad. Sci. USA* **97**, 12204–12209 (2000).
46. Abiru, N., Kawasaki, E. & Eguch, K. Current knowledge of Japanese type 1 diabetic syndrome. *Diabetes Metab. Res. Rev.* **18**, 357–366 (2002).
47. Ueda, H. *et al.* Association of the T-cell regulatory gene CTLA4 with susceptibility to autoimmune disease. *Nature*; advance online publication 30 April 2003/ doi 10.1038/nature01621.
48. Ranganath, S. *et al.* GATA-3-dependent enhancer activity in IL-4 gene regulation. *J. Immunol.* **161**, 3822–3826 (1998).
49. Afkarian, M. *et al.* T-bet is a STAT1-induced regulator of IL-12R expression in naive CD4+ T cells. *Nat. Immunol.* **3**, 549–557 (2002).
50. Hsieh, C.S. *et al.* Development of TH1 CD4+ T cells through IL-12 produced by Listeria-induced macrophages. *Science* **260**, 547–549 (1993).
51. Sha, W.C. *et al.* Selective expression of an antigen receptor on CD8-bearing T lymphocytes in transgenic mice. *Nature* **335**, 271–274 (1988).